

Superconductivity of the oxycarbonate $\text{Tl}_{0.5}\text{Pb}_{0.5}\text{Sr}_4\text{Cu}_2\text{CO}_3\text{O}_7$: A magnetic study

S. Peluau, A. Maignan, Ch. Simon, and A. Wahl

*Laboratoire CRISMAT, Institut des Sciences de la Matière et du Rayonnement, Université de Caen,
Boulevard du Maréchal Juin, 14050 Caen Cedex, France*

(Received 28 February 1994)

The magnetic behavior of the 71-K superconductor $\text{Tl}_{0.5}\text{Pb}_{0.5}\text{Sr}_4\text{Cu}_2\text{CO}_3\text{O}_7$, which consists of an intergrowth of the two nonsuperconducting phases $\text{Sr}_2\text{CuO}_2\text{CO}_3$ and $\text{Tl}_{0.5}\text{Pb}_{0.5}\text{Sr}_2\text{CuO}_5$, has been studied. Its pinning properties in terms of the critical current density J_c and the irreversibility line have been established using a modified-Bean-model expression for the magnetization data and compared to results for other thallium cuprates. Typical J_c was calculated to be $\sim 8 \times 10^6$ A/cm² at 5 K in a field of 0.2 T. The analysis of the reversible magnetization, leading to basic values of the parameters for this oxycarbonate as $\lambda_{ab}(0) = 170$ nm, $\xi_{ab}(0) = 2.39$ nm and $\kappa = 72.5$, was also performed. The latter values are compared to other existing data especially those concerning the thallium-based superconductors which have been derived from similar analyses. This study shows that the superconducting behavior of this oxycarbonate is closer to multiple copper layered cuprates than to the single copper layer "1201" phase although carbonate groups connect two successive copper layers. It can be considered as intermediate between the thallium bilayer cuprates and the best lead-doped "1223" and "1212" superconductors.

INTRODUCTION

The recent discovery of a series of superconductive copper oxycarbonates (see for a review Refs. 1 and 2), with T_c 's up to 80 K states the issue of the role of carbonate groups in superconductivity for these materials. This is especially the case of the 71-K superconductor $\text{Tl}_{0.5}\text{Pb}_{0.5}\text{Sr}_4\text{Cu}_2\text{CO}_3\text{O}_7$,³ which exhibits a rather sharp transition and a significant diamagnetic volume fraction of 65% in spite of the fact that its structure [Fig. 1(a)] consists of an intergrowth of two nonsuperconducting phases, $\text{Tl}_{0.5}\text{Pb}_{0.5}\text{Sr}_2\text{CuO}_5$ (Refs. 4 and 5) and $\text{Sr}_2\text{CuO}_2\text{CO}_3$.⁶⁻⁷ Thus, although this phase derives from that of the 1:2:0:1 cuprates [Fig. 1(b)] by replacing one $[\text{TlO}]_\infty$ layer out of two by rows of the carbonate groups, it appears as a much better superconductor.

A common feature of this oxycarbonate with the thallium cuprates deals with the anisotropy of its structure, which may induce, as in the latter a high anisotropy of its superconducting properties. The investigation of superconductivity in the thallium oxycarbonate is of capital importance, since it has been shown that the physical properties of most of the thallium cuprates exhibit low capacities to carry superconducting current at $T \gg 4.2$ K, so that their potential applications are limited. In particular, the positions of the irreversibility lines of such materials in the H - T plane are too low. Among the different thallium cuprates, it has been demonstrated that the monolayer ones exhibit better intrinsic pinning properties than the bilayers.^{8,9} A model, based on weak Josephson coupling of the CuO_2 layers between the rock-salt-type layers, has been proposed to explain such a difference; it predicts that the irreversibility line is steepened when the thickness of the rock-salt-type layers decreases.⁸ This may also explain the relatively good intrinsic pinning properties of the lead-based monolayer cuprate $\text{Tl}_{0.5}\text{Pb}_{0.5}\text{Sr}_2\text{Ca}_2\text{Cu}_3\text{O}_9$ abbreviated "TlPb-1:2:2:3".⁹⁻¹¹

For these reasons we have investigated the superconducting properties of the "TlPb" oxycarbonate $\text{Tl}_{0.5}\text{Pb}_{0.5}\text{Sr}_4\text{Cu}_2\text{CO}_3\text{O}_7$. Magnetic measurements have been performed on the corresponding ceramic. Pinning properties and characteristic superconducting parameters are derived here. These results are compared with exist-

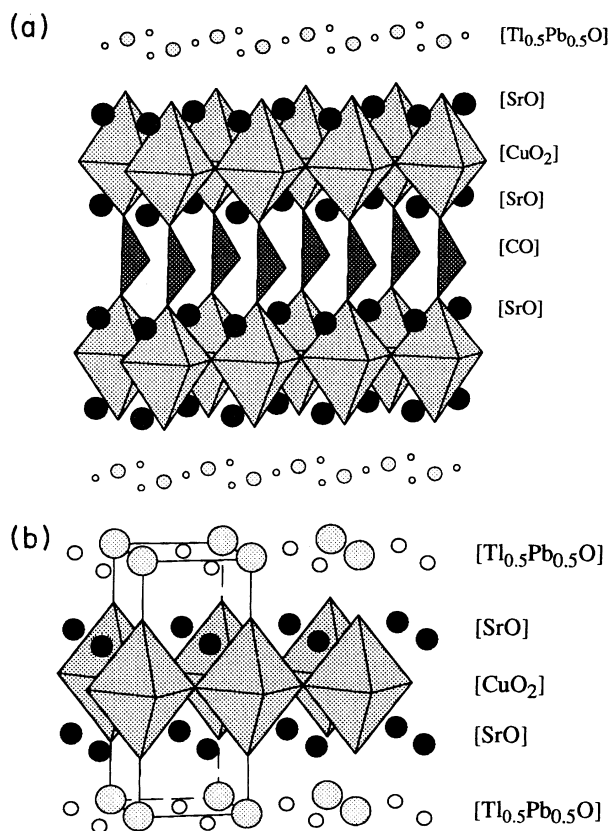


FIG. 1. Schematic structures of $\text{Tl}_{0.5}\text{Pb}_{0.5}\text{Sr}_4\text{Cu}_2\text{CO}_3\text{O}_7$ (a) and $\text{Tl}_{0.5}\text{Pb}_{0.5}\text{Sr}_2\text{CuO}_5$ (b).

ing data on the different thallium-based superconducting cuprates, especially with data determined by magnetization measurements on polycrystalline samples.

EXPERIMENTAL

A polycrystalline sample $Tl_{0.5}Pb_{0.5}Sr_4Cu_2CO_3O_7$ was prepared by the solid-state reaction method described in Ref. 3. In this technique, the reaction is carried out in a silica ampoule in order to prevent thallium losses oxides and CO_2 . The resulting product is an almost pure phase with some traces of $TlPb-1201$ and $SrCO_3$. As-synthesized samples are found to be superconductors with $20\text{ K} \leq T_c \leq 60\text{ K}$ and low-temperature annealings [290°C in argon-hydrogen flow (H_2 10%)] are performed in order to optimize T_c .³ The susceptibility versus temperature of the optimized compound in powder form is shown in Fig. 2.

In order to obtain basic superconducting parameters of this oxycarbonate, magnetic measurements were carried out using a superconducting quantum interference device (SQUID) magnetometer with field ranging from 0 to 5 T and temperature from 5 K to T_c . A pause of 600 s was applied after each magnetic-field settling when hysteresis loops were recorded in order to achieve good stability; a 2-cm scan length involving a small field inhomogeneity (0.1%) was chosen for the measurements. A capsule was filled with ~ 100 mg of oxycarbonate in powder form and fixed on the sample holder of the SQUID system. The mean size of the grains is $3\ \mu\text{m}$ as checked with a light-diffusion granulometer and the grains present plateletlike shapes as shown on the TEM microstructure of Fig. 3. The Curie-Weiss signal related to the impurities was measured above T_c to subtract from the experimental data. The diamagnetic volume fraction of 0.65 was taken into account to correct the magnetization data.

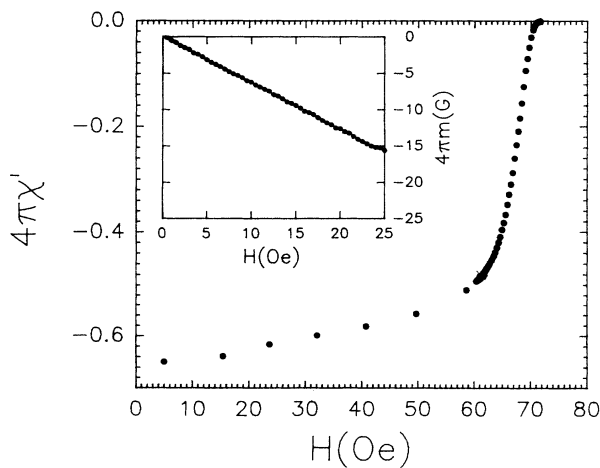


FIG. 2. Ac susceptibility versus temperature of $Tl_{0.5}Pb_{0.5}Sr_4Cu_2CO_3O_7$ ($H_{ac} = 80\text{ A m}^{-1}$, $f = 80\text{ Hz}$). In the inset the first magnetization versus applied magnetic field registered with a SQUID magnetometer at 5 K of the same sample is also given.

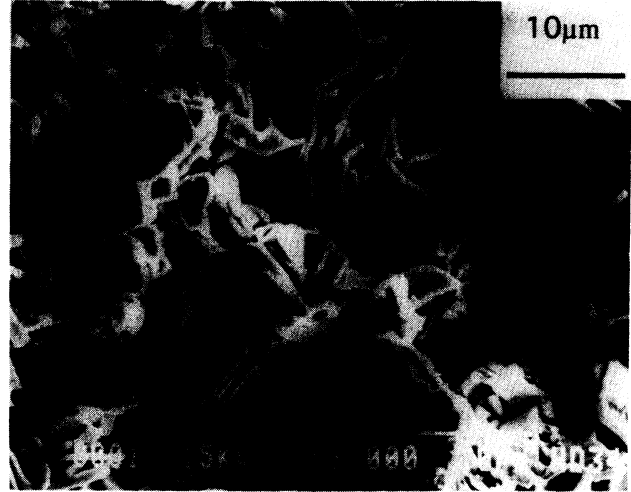


FIG. 3. TEM microstructure from a bar of $Tl_{0.5}Pb_{0.5}Sr_4Cu_2CO_3O_7$.

IRREVERSIBLE PROPERTIES

Magnetization loops at different temperatures were recorded in order to extract J_c values which are known to be strongly depressed by the temperature increase in thallium-based superconductors.¹² The Bean model modified for a polycrystalline sample was used with a grain size of $\sim 3\ \mu\text{m}$ to determine the limit of current flow in the individual grains. If one considers the anisotropy of such superconductors then J_c is mainly dominated by the $H||c$ component of the magnetization, and thus if θ is the angle between the magnetic-field direction and the c -axis direction of one grain of powder, then the magnetization difference $\Delta m(B) = m(B_+) - m(B_-)$ measured for all the grain assembly is related to the critical current density in the ab plane by the relation:

$$K \Delta m(B) = \int_0^{\pi/2} J_c(B \cos\theta) \cos\theta \sin\theta d\theta, \quad (1)$$

with $K = 30/d$ for platelet grains of mean diameter d in the Bean model. Equation (1) can also be written

$$B^2 \Delta m(B) = K^{-1} \int_0^B B' J_c(B') dB'$$

considering $B' = B \cos\theta$. Then,

$$J_c(B) = KB^{-1} \frac{d[B^2 \Delta m(B)]}{dB}. \quad (2)$$

This model for polycrystalline samples was successfully tested by a comparison with single crystals on $Tl_2Ba_2CaCu_2O_8$ and $Tl_2Ba_2Ca_2Cu_3O_{10}$. These results will be published elsewhere.

In Fig. 4(a), J_c values from Eq. (2) are presented in a semi-log plot with temperature ranging from 5 to 55 K. One can see that at low field and low temperature (5 K) J_c values reach a maximum of $\sim 8 \times 10^6\text{ A cm}^{-2}$; such data are typical of superconducting copper oxides. But in fact, as soon as the temperature increases, J_c falls off rapidly when the magnetic field increases.

In order to compare the classical Bean analysis and the

corrected one for grains of anisotropic superconductors [Eq. (2)], the corresponding sets of J_c 's at 40 K are reported in Fig. 4(b). In the inset is also shown the magnetization curve $m(H)$ at this temperature. This clearly establishes that J_c after correction is higher in the low-field region and also that corrected J_c decreases faster as H or T increases. This is also evidenced in Fig. 5 where the irreversibility lines B^* (defined as $J_c=0$ for $B > B^*$) versus reduced temperature t are represented and correspond to the same $J_c=10^4$ A cm $^{-2}$ criterion applied to J_c 's data obtained with or without correction of the Bean model. Experimental data of $B^*(t)$ for $\text{Tl}_{0.5}\text{Pb}_{0.5}\text{Sr}_2\text{Ca}_2\text{Cu}_3\text{O}_9$ from Ref. 13 are also reported; this irreversibility line corresponds also to a polycrystalline sample where no corrections have been performed. So the uncorrected $B^*(t)$ plot for the oxycarbonate is to be compared to the TIPb-1223 irreversibility line showing that $\text{Tl}_{0.5}\text{Pb}_{0.5}\text{Sr}_4\text{Cu}_2\text{CO}_3\text{O}_7$ pinning properties are less

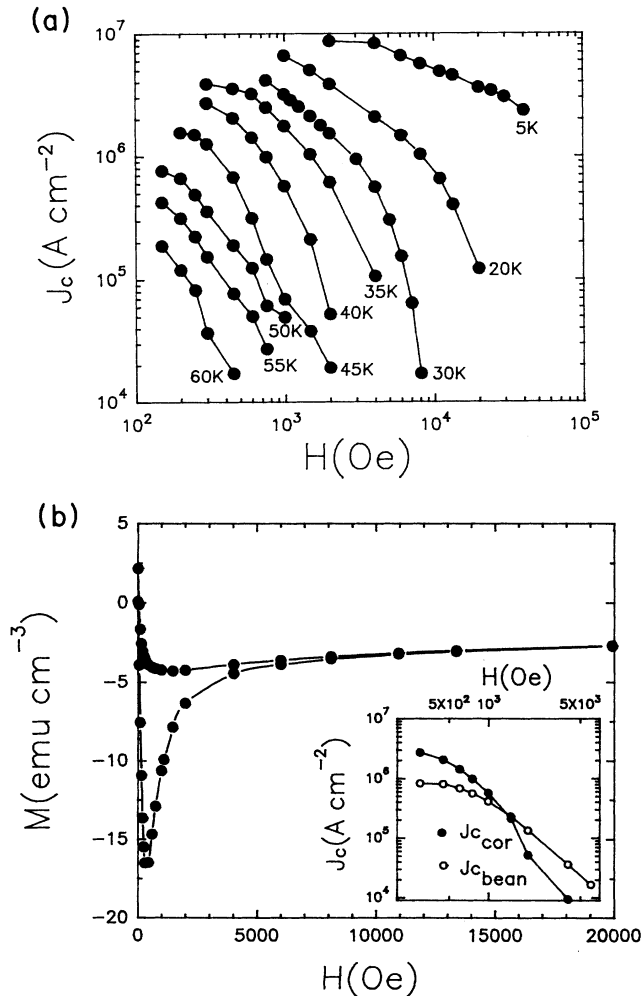


FIG. 4. (a) J_c values derived from magnetization versus field measurements at the different temperatures labeled on the graph. J_c 's are calculated with Eq. (2). (b) $J_c(H)$ at 40 K calculated with the classical Bean model and with the corrected one for a polycrystalline sample [Eq. (2)]. Inset the corresponding initial $m(H)$ loop registered at 40 K.

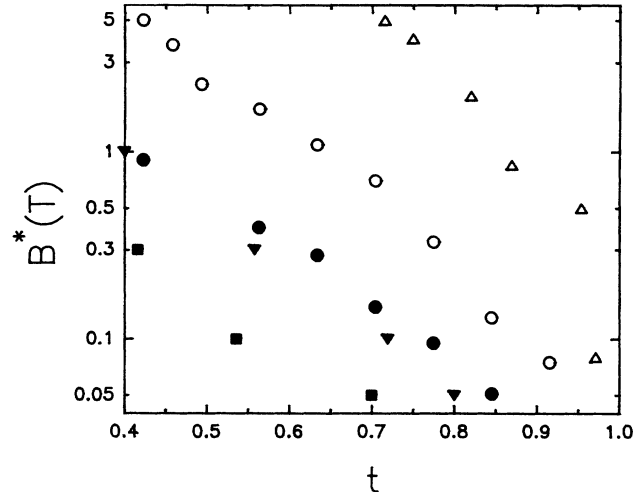


FIG. 5. Irreversibility lines $B^*(t)$ of $\text{Tl}_{0.5}\text{Pb}_{0.5}\text{Sr}_4\text{Cu}_2\text{CO}_3\text{O}_7$ extracted from $J_c(B)$ data with the Bean model (hollow circles) and with the corrected model (filled circles). $B^*(t)$ of polycrystalline $\text{Tl}_{0.5}\text{Pb}_{0.5}\text{Sr}_2\text{Ca}_2\text{Cu}_3\text{O}_9$ from Ref. 11 is also represented (hollow triangles) just as $B^*(t)$ of $\text{Tl}_2\text{Ba}_2\text{CaCu}_2\text{O}_8$ (filled squares) and $\text{Tl}_2\text{Ba}_2\text{Ca}_2\text{Cu}_3\text{O}_{10}$ (filled triangles) single crystals.

efficient. To our knowledge no irreversibility lines of TIPb-1223 single crystals have been reported. In order to compare the irreversibility line of the oxycarbonate after correction by our model the $B^*(t)$ curves of $\text{Tl}_2\text{Ba}_2\text{CaCu}_2\text{O}_8$ (“TI-2212”) and $\text{Tl}_2\text{Ba}_2\text{Ca}_2\text{Cu}_3\text{O}_{10}$ (“TI-2223”) single crystals¹⁴ are also reported in Fig. 5; the comparison shows that the oxycarbonate $B^*(t)$ line is higher in the (H, T) plane than the lines of the bilayer thallium cuprates.

It is remarkable that this oxycarbonate, which consists of single copper layers, exhibits a significantly higher irreversibility line than all the thallium bilayer cuprates whatever their structure of copper layers. Nevertheless its $B^*(t)$ line remains low compared to the thallium lead monolayer cuprates $\text{Tl}_{0.5}\text{Pb}_{0.5}\text{Sr}_2\text{Ca}_2\text{Cu}_3\text{O}_9$ (“TIPb-1223”) and $\text{Tl}_{0.5}\text{Pb}_{0.5}\text{Sr}_2\text{Ca}_{0.8}\text{Y}_{0.2}\text{Cu}_3\text{O}_7$ (“TIPb-1212”).⁹

REVERSIBLE PROPERTIES

The reversible part of the hysteresis loop, i.e., above the irreversibility line, provides a region in the (H, T) plane where the superconducting parameters can be extracted. In the intermediate-field region of $H_{c1} \ll H \ll H_{c2}$, the London model predicts a linear dependence of m upon $\ln H$ although minor corrections could be added as discussed by Hao *et al.*¹⁵ Recently, Zheng, Campbell, and Liu have used the latter analysis to extract basic superconducting parameters of two thallium-based compounds TIPb-1223 and TI-2223.¹⁶ Their results demonstrate that in the range of magnetic field 0–5 T the linear regime of $m(H)$ (Abrikosov formula) was never reached. So we have only considered the London model to fit our $m = f(\ln H)$ data applying a derived equation with κ and H_c as parameters:

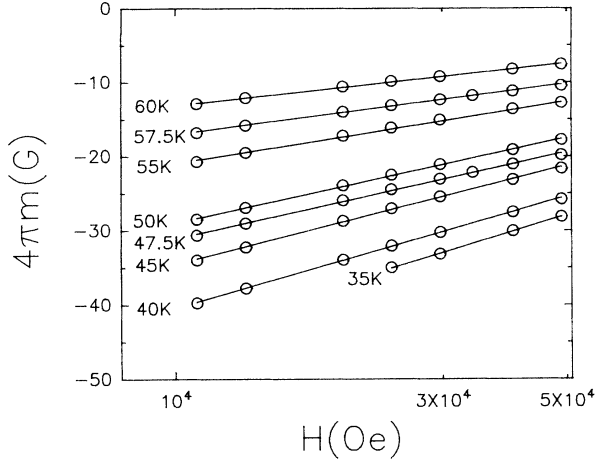


FIG. 6. Reversible magnetization m upon magnetic field H corresponding to the different temperatures indicated on the graph. The solid lines are fits obtained with Eq. (3).

$$m = \frac{H_c}{8\pi\sqrt{2}\kappa} \left[-\frac{1}{4} + \frac{1}{2} \ln \frac{H}{\beta\sqrt{2}\kappa H_c} \right]. \quad (3)$$

This expression derives from the London model expression

$$-4\pi m = \frac{\phi_0}{8\pi\lambda_{ab}^2} \ln \left[\frac{\beta H_{c2}}{H} \right] \quad (4)$$

with $\beta \sim 1.16$; considering the powder form of the sample, the latter relation must be corrected similarly to previous work on Tl-2223 and HgBa₂CuO₄ (Ref. 17) where the magnetization (m) was calculated for fully random crystallites yielding Eq. (3).

The experimental data $m = f(\ln H)$ and the associated fits with Eq. (3) are represented in Fig. 6. For each series

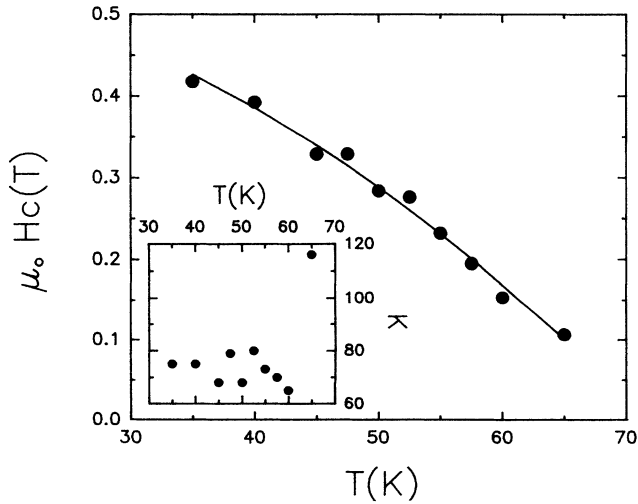


FIG. 7. Temperature dependence of H_c determined by fitting with Eq. (3) the reversible parts of the $m(H)$ plots with the average κ value of 72.5 [see also $\kappa(T)$ in the inset]. Solid line corresponds to the fit to Eq. (5).

TABLE I. Superconducting parameters of the oxycarbonate $Tl_{0.5}Pb_{0.5}Sr_4Cu_2CO_3O_7$ determined from magnetization data.

T_c (K)	$H_c(0)$ (T)	κ (average value)	$\frac{dH_{c2}}{dT}$ (T/K)	H_{c2} (T)	ξ_{ab} (nm)	H_{c1} (mT)	λ_{ab} (nm)
71	0.56	72.5	-1.2	57.6	2.39	24.4	170 188 ^a

^aFrom the slope calculations with formula of Eq. (6).

of data κ and H_c have been adjusted over a range of magnetic fields from 1 to 5 T. The resulting κ and H_c are reported in Fig. 7. This oxycarbonate exhibits an average κ value of 72.5 indicating the extreme type-II character of this superconductor. As described by Zheng, Campbell, and Liu,¹⁶ κ diverges close to T_c in the regime where fluctuations become important.

The $H_c(0)$ value was extrapolated using the empirical formula

$$H_c(T) = H_c(0) \left[1 - \left(\frac{T}{T_c} \right)^2 \right]. \quad (5)$$

Fitting with this formula (see Fig. 7) yields $T_c = 71.8$ K and $H_c(0) = 0.56$ T. The latter value is smaller than that of Tl-1223 and Tl-2223,¹⁶ which are, respectively, 0.92 and 0.79 T.

At this point of the analysis, $H_{c2}(0)$ can be derived since $H_{c2}(T) = \kappa\sqrt{2}H_c(T)$ leading to the slope $dH_{c2}/dT = -1.2$ T/K. Using the Werthamer, Helfand, and Hohenberg equation,¹⁸ an estimation of $H_{c2}(0)$ is obtained and consequently $\xi_{ab}(0)$, since $H_{c2}(0) = \phi_0/2\pi\xi_{ab}^2(0)$, where ϕ_0 is the flux quantum. Finally, one can also calculate $H_{c1}(0)$ and $\lambda_{ab}(0)$ from the relations $H_{c1}(0) = H_c(0) \ln \kappa / \sqrt{2}\kappa$ and $\sqrt{2}H_c(0) = \kappa\phi_0/2\pi\lambda_{ab}^2(0)$ using the average value for κ . All these data are summarized in Table I.

For the in-plane London penetration depth (λ_{ab}) determination, the slopes of the different $m = f(\ln H)$ curves

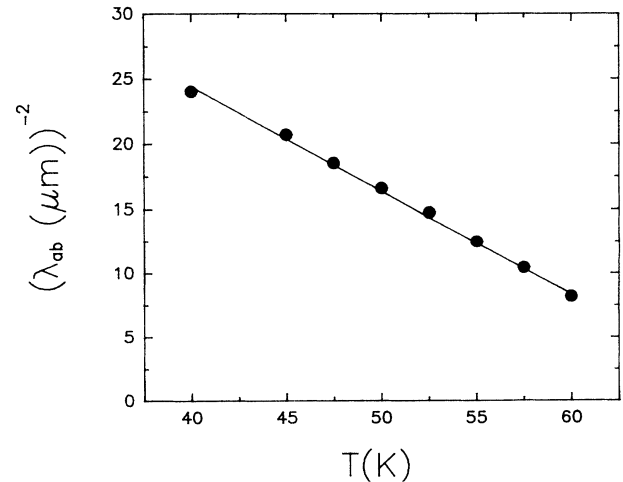


FIG. 8. λ_{ab}^{-2} versus T deduced from the $M - \ln H$ slopes with formula (6). Solid line is a fit with Eq. (7).

have also been computed considering the relation:

$$\frac{\delta(4\pi m)}{\delta \ln H} = \frac{\phi_0}{16\pi\lambda_{ab}^2(T)} \quad (6)$$

This method has been previously used to analyze reversible magnetization data of polycrystalline thallium cuprates Tl-2212 and Tl-2223.^{19,20} Our data are represented in the form λ_{ab}^{-2} versus T in Fig. 8. The straight line is a fit using the weak-coupling clean-limit expression:

$$\lambda_{ab}^{-2}(T) = 2\lambda_{ab}^{-2}(0) \times \left[1 - \frac{T}{T_c} \right] \quad (7)$$

with corresponding values $\lambda_{ab}(0) = 188$ nm and $T_c = 70.4$ K, this T_c value being very close to $T_c = 71$ K measured by ac susceptibility. Both $\lambda_{ab}(0)$ values for the oxycarbonate are very similar to those of Ref. 16 for Tl-2223 and TIPb-1223.

DISCUSSION

The central point of the study was to report for superconducting basic parameters of an oxycarbonate. When considering the data, the first remark concerns their good agreement with values previously published for superconducting cuprates. For instance, the value of $\lambda_{ab}(0) = 170$ nm is concordant with values reported for thallium cuprates. For these compounds a lot of data have already been published, ranging from ~ 110 to ~ 240 nm,^{14,16,17,19,20} these two extreme values correspond to Tl-2223 and derive from similar magnetic measurements. Our value is close to that of Zheng, Campbell, and Liu¹⁶ for TIPb-1223 ($\lambda_{ab} = 180$ nm). But the T_c value is 115 K for TIPb-1223, roughly ~ 50 K higher than that of the oxycarbonate. If one considers that in the clean limit the relation $\lambda^{-2} \propto n_s/m^*$ is valid and taking into account the relation $n_s/m^* \propto T_c$ deduced from μ SR measurements carried out on $\text{Ti}_2\text{Ba}_2\text{CuO}_{6\pm\delta}$ ("TI-2201") (Ref. 21) for different levels of hole doping, thus a λ_{ab} value close to that of TIPb-1223 may indicate that the T_c of the oxycar-

bonate is quite optimized.

Nevertheless, the mean κ value ($\kappa = 72.5$) is much smaller than κ of TIPb-1223 or Tl-2223 and corresponds to a larger $\xi_{ab}(0)$ value for the oxycarbonate ($\xi_{ab}(0) = 2.39$ nm) to be compared for instance to $\xi_{ab}(0) = 1.17$ nm for TIPb-1223. This major difference may be a consequence of the difference of T_c 's ($T_c = 71$ K for $\text{Tl}_{0.5}\text{Pb}_{0.5}\text{Sr}_4\text{Cu}_2\text{CO}_3\text{O}_7$ against $T_c = 115$ K for $\text{Tl}_{0.5}\text{Pb}_{0.5}\text{Sr}_2\text{Ca}_2\text{Cu}_3\text{O}_9$), since the superconducting gap Δ in BCS theory is proportional to ξ^{-1} and proportional to T_c . This is in agreement with the fact that $\text{La}_{1.85}\text{Sr}_{0.15}\text{CuO}_4$ exhibits a lower T_c value ($T_c = 35$ K) than the oxycarbonate ($T_c = 71$ K) but a larger $\xi_{ab}(0)$ value [$\xi_{ab}(0) = 32$ nm].²²

CONCLUSION

This set of data for the oxycarbonate $\text{Tl}_{0.5}\text{Pb}_{0.5}\text{Sr}_4\text{Cu}_2\text{CO}_3\text{O}_7$ clearly demonstrates the original character of this superconductor. This material that is characterized like the 1201 cuprates by thallium monolayers, exhibits much higher T_c and pinning properties that are intermediate between those of bilayer thallium cuprates and those of the best monolayer lead-doped thallium "TIPb-1223" cuprates. Consequently this thallium lead oxycarbonate behaves more like a multiple copper layer cuprate rather than a single copper-layer phase. Thus the study of superconducting oxycarbonates is of importance especially for the prospect of new high- T_c materials and for the understanding of superconductivity. A comparison with other oxycarbonates is now in progress particularly with $\text{TlBa}_2\text{Sr}_2\text{Cu}_2\text{CO}_3\text{O}_7$ ($T_c = 62$ K) whose modulated structure derives also from the 1201-type.²³

ACKNOWLEDGMENTS

The authors thank Professor B. Raveau for valuable discussions. Laboratoire CRISMAT is Unité de Recherche Associée au CNRS No. 1318.

¹B. Raveau, M. Huvé, A. Maignan, M. Hervieu, C. Michel, B. Domengès, and C. Martin, *Physica C* **209**, 163 (1993).

²C. Michel, M. Hervieu, C. Martin, A. Maignan, B. Domengès, and B. Raveau, in *Proceedings of the 5th International Conference on Superconducting Materials*, Paris, 1993, edited by J. Etourneau, J. B. Torrance, and H. Yamauchi (IIT-International, Paris, 1993), pp. 15–21.

³M. Huvé, C. Michel, A. Maignan, M. Hervieu, C. Martin, and B. Raveau, *Physica C* **205**, 219 (1993).

⁴C. Martin, D. Bourgault, C. Michel, J. Provost, M. Hervieu, and B. Raveau, *Eur. J. Inorg. Solid State Chem.* **26**, 1 (1989).

⁵M. H. Pan and M. Greenblatt, *Physica C* **176**, 80 (1991).

⁶Y. Miyazaki, H. Yamane, T. Kajitani, T. Oku, K. Higara, Y. Morii, K. Fuchizaki, S. Funahashi, and T. Hirai, *Physica C* **191**, 434 (1992).

⁷A. R. Armstrong and P. P. Edwards, *J. Solid State Chem.* **98**, 432 (1992).

⁸D. H. Kim, K. E. Gray, R. T. Kampwirth, J. C. Smith, D. S.

Richeson, T. J. Marks, J. H. Kang, J. Talvacchio, and M. Eddy, *Physica C* **177**, 431 (1991).

⁹M. R. Presland, J. L. Tallon, N. E. Flower, R. G. Buckley, A. Mawdsley, M. P. Staines, and M. G. Fee, *Cryogenics* **33**, 502 (1993).

¹⁰K. Aihara, T. Doi, A. Soeta, S. Takeuchi, T. Yuasa, M. Seido, T. Kamo, and S. Matsuda, *Cryogenics* **32**, 936 (1992).

¹¹R. S. Liu, D. N. Zheng, J. W. Loram, K. A. Mirza, A. M. Campbell, and P. P. Edwards, *Appl. Phys. Lett.* **60**, 1019 (1992).

¹²A. P. Malozemoff, *Physical Properties of High Temperature Superconductors I*, edited by D. M. Ginsberg (World Scientific, Singapore, 1989), p. 71.

¹³T. Yuasa, T. J. Doi, A. Soeta, N. Inoue, K. Aihara, T. Kamo, and S. P. Matsuda, *Jpn. J. Appl. Phys.* **31**, L1176 (1992).

¹⁴A. Maignan, C. Martin, V. Hardy, Ch. Simon, M. Hervieu, and B. Raveau, *Physica C* **219**, 407 (1994).

¹⁵Z. Hao, J. R. Clem, M. W. Mc Elfresh, L. Civale, A. P. Maol-

- zemoff, and F. Holtzberg, *Phys. Rev. B* **43**, 2844 (1991).
- ¹⁶D. N. Zheng, A. M. Campbell, and R. S. Liu, *Phys. Rev. B* **48**, 6519 (1993).
- ¹⁷J. R. Thompson, J. G. Ossandon, D. K. Christen, B. C. Chakoumakos, Y. R. Sun, M. Paranthaman, and J. Brynestad, *Phys. Rev. B* **48**, 14 031 (1993).
- ¹⁸N. R. Werthamer, E. Helfand, and P. C. Hohenberg, *Phys. Rev. B* **147**, 295 (1966).
- ¹⁹A. Schilling, F. Hulliger, and H. R. Ott, *Z. Phys. B Condens. Matter* **82**, 9 (1991).
- ²⁰J. R. Thompson, D. K. Christen, H. A. Deeds, Y. C. Kim, J. Brynestad, S. T. Sekula, and J. Budai, *Phys. Rev. B* **41**, 7293 (1990).
- ²¹Y. J. Uemura, A. Keren, L. P. Le, G. M. Luke, W. D. Wu, Y. Kubo, T. Manako, Y. Shimikawa, M. Subramanian, J. L. Cobb, and J. T. Markert, *Nature (London)* **364**, 605 (1993).
- ²²Q. Li, M. Suenaga, T. Kimura, and K. Kishio, *Phys. Rev. B* **47**, 11 384 (1993).
- ²³F. Goutenoire, M. Hervieu, A. Maignan, C. Michel, C. Martin, and B. Raveau, *Physica C* **210**, 359 (1993).

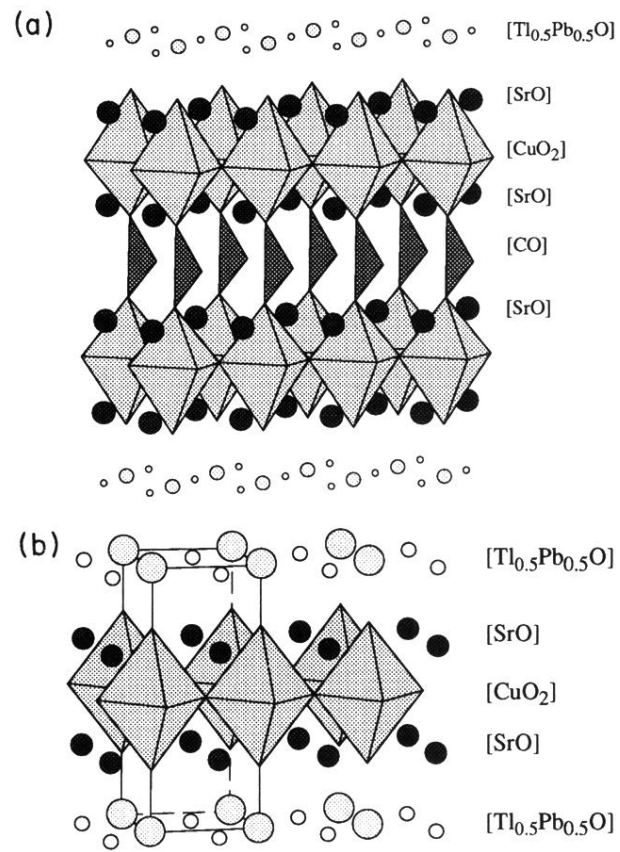


FIG. 1. Schematic structures of $\text{Tl}_{0.5}\text{Pb}_{0.5}\text{Sr}_4\text{Cu}_2\text{CO}_3\text{O}_7$ (a) and $\text{Tl}_{0.5}\text{Pb}_{0.5}\text{Sr}_2\text{CuO}_5$ (b).

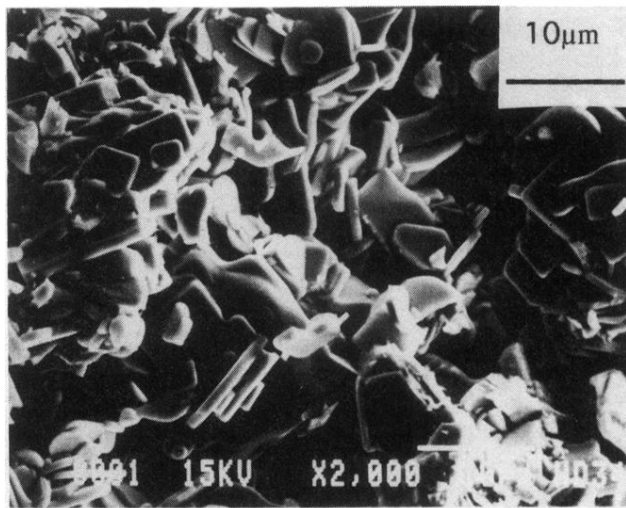


FIG. 3. TEM microstructure from a bar of $\text{Tl}_{0.5}\text{Pb}_{0.5}\text{Sr}_4\text{Cu}_2\text{CO}_3\text{O}_7$.